Numerical analysis of transonic flow over a rectangular cavity

Akshay Khare
Mechanical and Aerospace Engineering
IIT Hyderabad
Hyderabad, India
me23mtech14002@iith.ac.in

Amartya Jana
Hornbill Aerospace and Defence Pvt. Ltd.
Hyderabad, India
janaamartya@gmail.com

Rutuja Patil
Mechanical and Aerospace Engineering
IIT Hyderabad
Hyderabad, India
me24mtech14006@iith.ac.in

Mahesh M. Sucheendran
Mechanical and Aerospace Engineering
IIT Hyderabad
Hyderabad, India
mahesh@mae.iith.ac.in

doi: https://doi.org/10.37285/bsp.SACAD2025.27

***Abstract*—The noise generated from transonic air flow over a rectangular cavity has been of importance to multitude of engineering applications. This study investigates the acoustic behavior of a such cavity using a hybrid Large Eddy Simulation (LES) approach named Improved Delayed Detached Eddy Simulations (IDDES). The aim is to predict the resulting sound pressure levels and understand the physics of noise generation from an in-depth study of the flow dynamics. Major aspects of the flow dynamics for example the shear layer fluctuations, shock propagation, and recirculation inside the weapon bay are examined from the results of numerical simulations. The present numerical results are also validated against the existing data obtained from previous experiments. Further, the resulting noise levels and the corresponding frequencies are calculated to understand the major sources of noise. *Index Terms*—Aero-acoustics, cavity noise, noise control.**

I. Introduction

Noise generation from transonic flow over a rectangular cavity is routinely encountered in different engineering problems. Two common instances are the weapon bay and the landing gear bay in military and civil aircraft. In all modern aircraft, the landing gears are kept inside a cavity to reduce the drag during its flight time and also, in the combat aircraft, weapons are stored inside similar cavities to reduce both the drag and radar signature. However, when the flow passes over these cavities, it creates strong unsteady aerodynamic effects leading to significant noise and pressure oscillations. These can damage internal components or aircraft structures, and also produce sound levels as high as 170 dB. This profoundly exacerbates the stealth properties of the aircraft in a military mission. The primary challenge here is to keep the noise levels under a recommended value without abandoning the desired aerodynamic qualities of the aircraft. Over the past years, several measures were taken to meet the operational standards, and the efficacy of these measures was verified with experiments and numerical simulations. Nonetheless, a comprehensive understanding of the effects of transient flow dynamics on the noise generation is still to be apprehended fully. Especially, the oscillations of the shear layer over the cavity and its dynamic interactions with the ensuing shock and expansion waves play a crucial role in the noise generation in the transonic regime. During the initial transients of the cavity door opening, these effects become profound. The aggravation of shear layer fluctuations with the onset of shock waves becomes the dominant source of higher sound pressure levels from the cavity. The shock wave breaks the turbulent shear layer into smaller turbulent structures which bring about highly non - steady pressure oscillations into the cavity. This suffices a highly accurate analysis in both space and time to resolve the underlying physics of the flow evolution and noise generation.

High-speed transonic or supersonic airflow inside cavities like weapon bays and landing gear bays creates loud noise, turbulence, and flow fluctuations. This has become a practical challenge for the stealth operation of a combat aircraft [1]. Historically, the first scientific measurements of air flowing over a cavity were presented by Roshko [2]. He chose low Mach number flows over cavities of varying dimensions. The pressure and velocity were measured at various points on the cavity wall. The author also demonstrated the differences in the ensuing vortex structures inside shallow and deep cavities. During the same time, Owen [3] and Rossiter [4] also conducted wind tunnel testing of the flow over cavities at the Royal Aircraft Establishment (RAE). They demonstrated different techniques to measure the pressure fluctuations inside the cavity. Further, Rossiter proposed a semi-empirical relation to determine the major frequencies of noise from a cavity flow. Krishnamurthy [5] conducted experimental measurements and flow visualizations to explore the mechanism of noise generation from a cavity. The experiments were conducted at the wind tunnel facility in the Jet Propulsion Laboratory of the California Institute of Technology. The author found a critical length of cavity for the onset of noise generation. The effect of shear layer apply on the noise was explained at length. Plumblee et al. [6] varied the flow Mach number from subsonic to high supersonic range $(0.2-5)$ to study the effect of shock and expansion waves on the resulting acoustic signal from the cavity. The researchers found that the acoustic signal from the trailing edge exhibited distinct frequencies, whereas the higher sound pressure levels were obtained at the leading edge. East [7] studied the aerodynamic sources of noise generated by the air flowing over a rectangular cavity. The noise distribution exhibited distinct frequencies, which were correlated to the size and shape of the cavity. The author observed swirling vortices in the flow field as the high-speed air was passing the cavity. The vortices were convected with the mean flow, and impacts the rear edge of the cavity. The impact produced acoustic waves that got reflected back towards the leading edge. These reflected waves disturbed the air and created a cycle of pressure fluctuation inside the cavity. This repetitive flow phenomenon gave rise to some distinct frequencies in the resulting acoustic signal. Heller et al. [8] Conducted experiments of flow over a rectangular cavities of varying length to depth ratios $(4-7)$. The researchers concluded that the maximum peak acoustic noise was obtained near the trailing edge of the cavity, and it gradually decreased towards the leading edge.

With the rapid progress of scientific computational facilities, researchers and engineers employed high- performance computations to delve into the details of highly complex flows. Transient flow structures of varying geometric scales can be resolved with a high degree of accuracy with these computations. In the earlier attempts to predict the acoustic signals from cavity flows, the works of Shih et al. [9] and Zhang et al. [10] revealed that the Unsteady Reynolds-Averaged Navier-Stokes (URANS) formulation failed to capture some of the intrinsic aspects of the phenomenon. Alternatively, evolutions of a wide range of vortex structures can be simulated with sophisticated LES-based turbulent models. The LES was employed to predict the cavity acoustics of supersonic weapon bay flows by Smith et al. [11] and aeronautical optical deep cavities by Larcheveque et al. [12] [13]. Crook et al. [14] employed a Large-Eddy Simulation (LES) based model to simulate the airflow over a deep cavity. The major frequencies of noise and the vortex dynamics were captured with remarkable accuracy. Though the LES-based approaches could simulate the large scale energy containing eddies with remarkable accuracy, the smaller scales near the walls required a finer resolution. The computational cost rose quite significantly. Recently, some alternative hybrid RANS-LES approaches have been adopted in practical applications to obtain satisfactory level of accuracy at a moderate computational cost. The near-wall turbulence is solved with a prescribed RANS solver, and the LES model is employed in the regions away from the wall. Such a turbulence model was proposed by Shur [15], which is known as the Improved Delayed Detached Eddy Simulations (IDDES). This model has been employed in the present numerical study.

In this work, the IDDES is adopted to simulate the flow over a weapon bay in transonic conditions. The study further predicts the sound pressure levels from the unsteady pressure fluctuations obtained from the numerical simulations. The goal is to understand the main sources of noise resulting from the unsteady flow variables. With this respect, the transient behavior of the turbulent shear layer and its interactions with the shock and expansion waves at the transonic regime are thoroughly investigated. This suffices the need to capture the turbulent flow structures of varying scales with sufficient resolution. The grid resolutions and computational techniques necessary for the present analyses are also reviewed in detail. Finally, the origin of the major frequencies of noise are explained from these flow phenomena. Remaining part of the article is organized as follows. In the following section, an overview of the computational domain and the numerical procedures are described. The results of flow dynamic simulations will be elaborated next. In the conclusion, the major findings and the possible future directions of this study are presented.

II. Methodoloy

The essential details of the numerical approach used to predict the acoustic field and sound pressure levels within the rectangular cavity is outlined in this section. All the numerical simulations have been performed with a commercial Finite Volume Method (FVM) solver, CFD++ of METACOMP Technology. The simulations are executed with a parallel computing facility with 300 processors. The full details of the geometry, flow properties, and boundary conditions is provided here.

A. *Problem definition*

The numerical simulations are conducted over a rectangular cavity with a length-to-depth ratio (L/D) of 5 and a width-to-depth (W/D) ratio of 1. The inflow conditions correspond to a Reynolds number (Re) of 1×10^6, based on the cavity length (L). Simulations are carried out at three transonic Mach numbers, $M = 0.85, 0.98$, and 1.19. The domain used for the computations and the corresponding boundary conditions are shown in Figure (**??**). The domain is carefully sized to minimize the pressure waves reflected at the boundaries. The upstream section extends from the cavitys leading edge towards the inlet boundary, ensuring an undisturbed boundary layer growth over the trailing surface of the cavity. Frictionless wall condition is implemented in this region to ensure an undisturbed inflow till the trailing surface of the cavity. The upstream boundary face is defined as the inlet, and the outlet boundary is placed far downstream of the flow domain. The distance between far-field boundary and cavity is 2540 mm, where the free stream conditions prevail. All the primitive variables such as velocities (u, v, w), static pressure (p), static temperature (T) and density are prescribed at the inlet and outlet boundaries ($p = 101325$ Pa, $T = 300$ K, and $u = 295$ m/s). The no-slip impenetrable viscous wall boundary conditions are enforced on the walls of the cavity. Appropriate symmetry boundary conditions are implemented on the front and rear boundaries of the flow domain (see Figure 1).

B. *Domain discretization*

In this study, the turbulent structures and fluctuating flow variables are simulated with the IDDES model, which entails sufficient refinement of the computational grid at certain locations of particular interest. For a standard LES-based turbulent flow simulation, it is imperative that 80% of the larger eddies must be resolved with the existing mesh, and the remaining smaller eddies are modeled with a suitable Sub-grid Scale model (SGS). Therefore, a region of very fine mesh has been introduced around the cavity. This region is deemed to be influenced by the turbulence and multiple wave-propagations such as shock and acoustic waves. Therefore, the average size of a finite volume cell has been taken as $0.1mm$ there. Additionally, the viscous boundary layers next to the walls have been captured with finer inflation

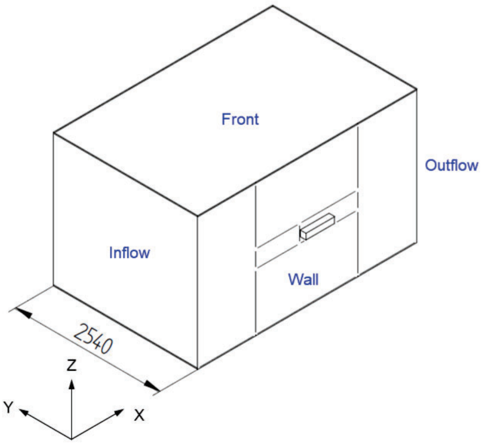

(a) Three dimensional view of the domain

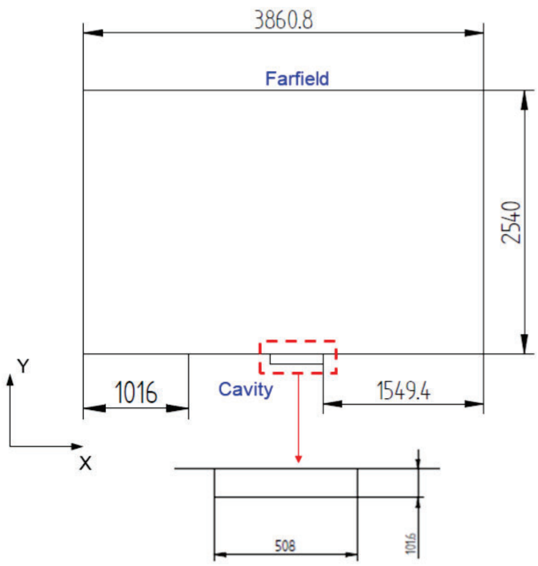

(b) Cut section view in the XY plane

Fig. 1: The flow domain with the corresponding boundaries (units shown here are in mm)

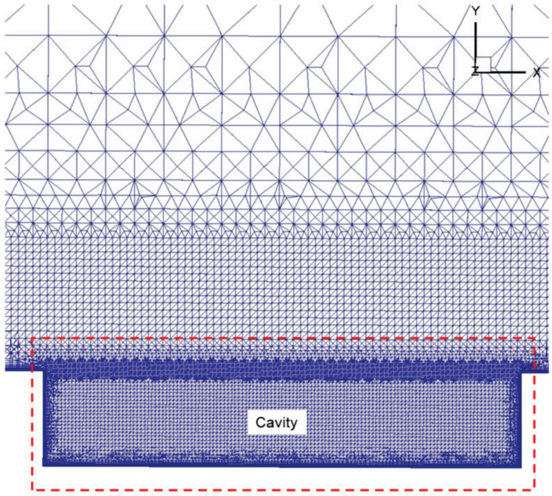

(a) Cut section in the XY plane

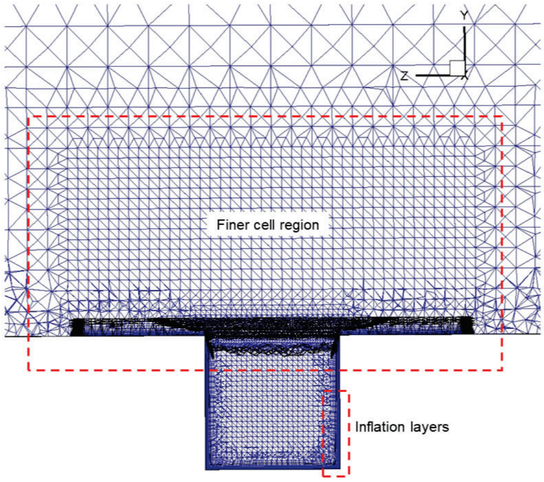

(b) Cut section in the YZ plane

Fig. 2: Planar view of the computational domain with different cell regions

layers, where the first layer of cells are given a height of $1 \times 10^{-2}mm$ normal to the wall surface. This ensures that the nondimensional y^+ values are maintained at 1, approximately. With these intricacies, the entire flow domain has been discretized with a total number of 5.1×10^6 unstructured cells. The discretized flow domain along with the regions of particular interest is shown in Figure 2.

C. Numerical procedure

To simulate the turbulent flow over the cavity, the IDDES method is adopted as the solution strategy. IDDES operates as a hybrid of RANS and LES methods with an improved strategy to resolve multiple scales of turbulent flows. The IDDES model evolved from the well known Delayed Detached Eddy Simulation (DDES) method, another hybrid turbulence model. In this approach, the RANS based Spalart-Allmaras (S-A) $1-$equation model is applied in the attached boundary layer, while the LES is used to simulate the separated flow regions, typically away from the solid boundary.

Detached Eddy Simulation (DES) is one of the hybrid turbulence models, where the RANS $1-$ equation SA model is used in the attached boundary layer and the rest of the domain is solved with the LES approach. In DES, the length scale switches between the RANS and LES as following.

$$l_{DES} = min(l_{RANS}, l_{LES}) \tag{1}$$

Here, $l_{RANS} = d$. d is the normal distance from the wall. l_{LES} is the length scale calculated from the calculated thickness of the viscous boundary layer (δ). Therefore, within the viscous sublayer, the RANS solution will be invoked. The model switches to LES as $d > \delta$.

The Delayed Detached Eddy Simulation (DDES) model was later introduced to overcome some of the shortcomings of the DES approach. In DDES modified as following.

$$l_{DDES} = l_{RANS} - f_d max(0, l_{RANS}, l_{LES}) \tag{2}$$

$$f_d = 1 - tanh([g_{rd}^2]) \tag{3}$$

$$g_{rd} = \frac{\nu + \nu_t}{k^2 d^2 (\frac{\partial u_i}{\partial x_j})(\frac{\partial u_i}{\partial x_j})} \tag{4}$$

Where ν and ν_t are the molecular and turbulent eddy viscosity, respectively, and κ is the Krmn constant. The delay function f_d is designed so that it equals 1 in the logarithmic law region and decreases smoothly toward zero at the edge of the boundary layer, ensuring a positive value for r_d. The switching criterion for DDES is written below.

$$l_{DDES} = \begin{cases} l_{RANS}, & \text{if } f_d = 0 \text{ and } r_d > 1 \\ l_{DES}, & \text{if } f_d = 1 \text{ and } rd \ll 1 \end{cases} \tag{5}$$

Wall Modeling in LES (WMLES) uses RANS approach within a much thinner region near the wall, where the wall distance is much smaller than the thickness of the boundary layer (δ). The effective length scale for this combined RANS and LES approach is shown below.

$$l_{WMLES} = f_B(1 + f_e)l_{RANS} + (1 - f_B)l_{LES} \tag{6}$$

Where f_B and f_e are blending functions that control the transition between RANS and LES. The blending function f_B is expressed as, $f_B = min(2e^{-3d/h}, 1)$, with $a = 0.25 - \frac{d}{h}$. It varies from 0 to 1 ensuring a rapid transition between RANS ($f_B = 1$) and $LES(f_B = 0)$ modes within a range of $0.5h < d < h$. The elevating function f_e is given by:

$$f_e = mxa(f_{e1} - 1, 0)\psi f_{e2} \tag{7}$$

This prevents excessive reduction of the RANS based turbulent stresses. This is particularly important in the interaction region near the RANS-LES interface, where it also helps resolving log-layer mismatch issues. The functions f_{e1}, f_{e2}, and ψ depend on $\frac{d}{h}$. IDDES offers a better treatment for both near-wall and separated turbulence in complex simulations. The Improved Delayed Detached Eddy Simulation (IDDES) is an advanced turbulence model used in CFD. It smartly switches between two methods: DDES (Delayed Detached Eddy Simulation) for detached flow regions, and WMLES (Wall-Modeled Large Eddy Simulation) for wall-attached regions.

$$l_{IDDES} = \bar{f}_d(1 + f_e)l_{RANS} + (1 - \bar{f}_d)l_{LES} \tag{8}$$

Where $\bar{f}_d$ and f_e are blending and elevating functions, respectively, and l_{RANS} and l_{LES} represent the characteristic length scales for RANS and LES regions.

$$l_{IDDES} = \begin{cases} l_{IDDES} = \bar{d}l_{RANS} + (1 - \bar{f}_d)l_{LES}, & \text{if } f_e = 0 \\ l_{WMLES} = f_B(1 + f_e)l_{RANS} + (1 - f_B)l_{LES}, & \text{If} f_e > 1 \end{cases} \tag{9}$$

The variable r_{dt} is derived from the SpalartAllmaras turbulence model.

D. Validation

The results of the present numerical study were verified against experimental and numerical data published earlier. Sound Pressure Levels (SPL) at different points were compared with the previous LES and experimental Particle Image Velocimetry (PIV) results. SPL values were calculated from the pressure fluctuation signals obtained from the numerical simulations. The numerical pressure values are probed at ten prescribed locations along the cavity according to an earlier experimental work [16] (see Figure 3). The peak frequencies closely match the values available in literature .

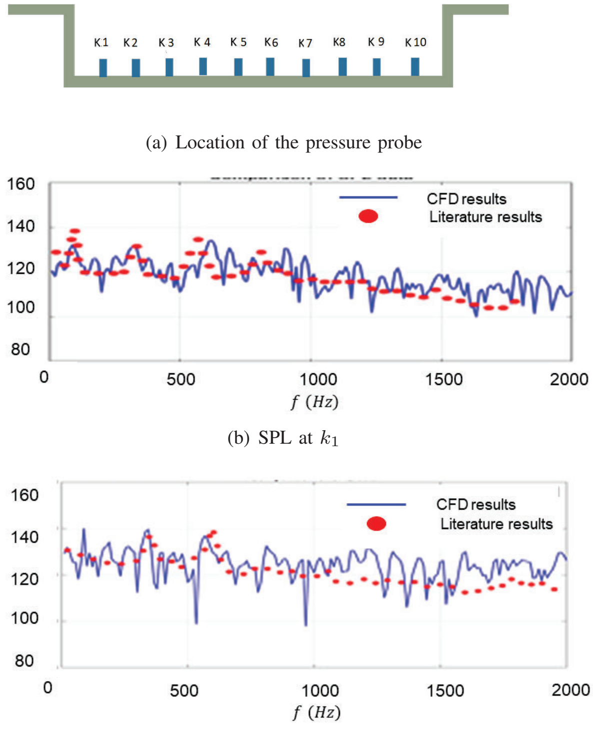

(a) Location of the pressure probe

(b) SPL at k_1

(c) SPL at k_6

Fig. 3: Comparison of the major frequencies obtained from the present numerical study with literature values [16]

III. Results and discussion

As discussed previously, the mechanism of noise generation is primarily governed by the complex interactions of turbulence and shock and expansion waves ensuing in the flow domain. The propagation of shock wave along the cavity, and its effects on the turbulent structures can be observed from the numerical schlieren and the corresponding contours of normal vorticity on a specified plane of the flow domain. Figure 4 demonstrates the dynamic phenomenon during the starting stages of the flow evolution. In the first instant ($t = 0.5ms$) a large vortex resulting from the flow recirculation near the trailing edge of the cavity, whereas the flow close to the leading edge remains largely non-turbulent (see Figure **??**). Though, a strong reflected shock wave (Figure **??**) is found to traverse upstream. At a later instant ($t = 3ms$) the reflected shock strongly interacts with the vortices at the trailing edge leading to a highly turbulent flow into the cavity.

With the combined effects of shock and turbulence, the flow field into the cavity grows highly unsteady, which can be perceived from the time-varying pressure at three different locations inside the cavity. Figure 5 shows pressure variations at the three chosen locations (k_1, k_2, and k_3). The amplitudes of pressure oscillations at the trailing edge are significantly lower than those at the leading edge. Distinct pressure spikes can be observed at the leading edge of the cavity. These high-pressure spikes at the leading edge are resulting from the shock and expansion waves ensuing there. The spatial distributions of Mach number along the flow domain in Figure 5 also reveal this. The initial expansion at the leading edge of

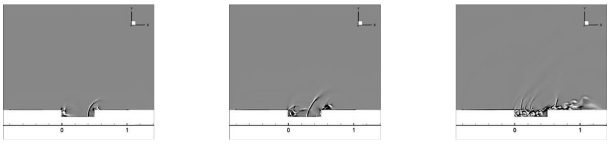

(a) time= $0.5ms$ (b) time= $1ms$ (c) time= $3ms$

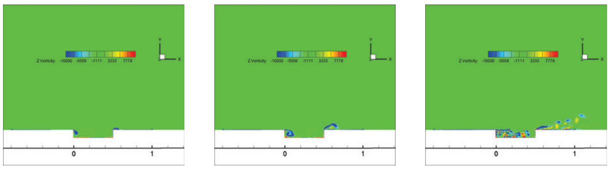

(d) time= $0.5ms$ (e) time= $1ms$ (f) time= $3ms$

Fig. 4: Numerical schlieren and contours of Z component of vorticity along the XY plane

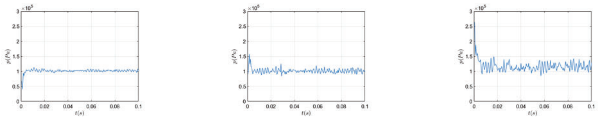

(a) At k_1 (b) At k_6 (c) At k_{10}

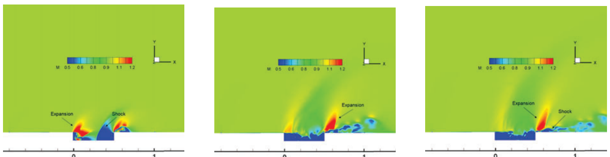

(d) time= $1ms$ (e) time= $3ms$ (f) time= $4ms$

Fig. 5: Temporal variations of pressure at three prescribed locations inside cavity

the cavity gradually dwindles with time. Whereas, the trailing edge remains susceptible to shock and expansion waves at the later stages as well. The low-amplitude fluctuations along the trailing edge originate from the unsteady vortices, which mostly contribute to the broadband noise. Whereas, the high-pressure fluctuations in the trailing edge give rise to distinct tones with higher SPL in the acoustic signal from the cavity.

The effect of inflow Mach number can further be elaborated by comparing the Overall Sound Pressure Levels (OASPL) along the center line for the cavity (Figure 6). For each Mach number in the transonic regime, the unsteady pressure fluctuations at the front ($\frac{X}{L} = 0.05$) and rear ($\frac{X}{L} = 0.95$) edge of the cavity floor are recorded. The dimensionless pressure fluctuation is defined as $p' = \frac{(p-\bar{p})}{p_\infty}$, where p and $\bar{p}$ are the instantaneous and mean pressures, respectively, and p_∞ is the free-stream pressure. This analysis shows that an increase in Mach number results in a higher OASPL in the cavity.

IV. Conclusion

Essential features of the aerodynamics and acoustics of a rectangular cavity (eg. weapon bay of a combat aircraft or landing gear) are studied at the transonic regime. Sophisticated LES-based numerical simulations have been conducted to analyze the high-speed turbulent flow field and the mechanisms of noise generation therein. Three different Mach numbers (0.85, 0.98, and 1.19) in the transonic regime were considered. The results showed marked difference in the acoustic signals obtained at the two extreme edges of the rectangular cavity. The leading edge mostly contributes to that broadband noise, whereas the trailing edge give rise to distinct peaks of higher SPL in the acoustic signal. This signals to a frequent occurrence of shock and expansion waves at that location. The OASPL inside the cavity also increases with Mach number due to a stronger shock interactions. These findings are supported by the earlier experimental and numerical findings.

References

[1] S. Lawson and G. Barakos, "Review of numerical simulations for high-speed, turbulent cavity flows," *Progress in Aerospace Sciences*, vol. 47, no. 3, pp. 186–216, 2011.
[2] A. Roshko, "Some measurements of flow in a rectangular cutout," Tech. Rep., 1955.
[3] T. B. Owen, "Techniques of pressure-fluctuation measurements employed in the rae low-speed wind-tunnels," Tech. Rep., 1958.
[4] J. Rossiter, "Wind-tunnel experiments on the flow over rectangular cavities at subsonic and transonic speeds," 1964.
[5] K. Krishnamurty, "Sound radiation from surface cutouts in high speed flow," Ph.D. dissertation, California Institute of Technology, 1956.
[6] H. Plumblee, J. Gibson, and L. Lassiter, *A theoretical and experimental investigation of the acoustic response of cavities in an aerodynamic flow*. Flight Dynamics Laboratory, Aeronautical Systems Division, Air Force Systems , 1962, vol. 61.
[7] L. East, "Aerodynamically induced resonance in rectangular cavities," *Journal of Sound and Vibration*, vol. 3, no. 3, pp. 277–287, 1966.
[8] H. H. Heller, D. Holmes, and E. E. Covert, "Flow-induced pressure oscillations in shallow cavities," *Journal of Sound and Vibration*, vol. 18, no. 4, pp. 545–553, 1971.
[9] S. Shih, A. Hamed, and J. Yeuan, "Unsteady supersonic cavity flow simulations using coupled k-epsilon and navier-stokes equations," *AIAA Journal*, vol. 32, no. 10, pp. 2015–2021, 1994.
[10] X. Zhang and J. Edwards, "Computational analysis of unsteady supersonic cavity flows driven by thick shear layers," *The Aeronautical Journal*, vol. 92, no. 919, pp. 365–374, 1988.
[11] B. R. Smith, "Large eddy simulation of a supersonic cavity flow with an unstructured grid flow solver," 2001.
[12] L. Larchevêque, P. Sagaut, I. Mary, O. Labbé, and P. Comte, "Large eddy simulation of a compressible flow past a deep cavity," *Physics of Fluids*, vol. 15, no. 1, pp. 193–210, 2003.
[13] L. Larcheveque, P. Sagaut, and T.-H. Lê, "Large eddy simulations of flows in weapon bays," in *41st Aerospace Sciences Meeting and Exhibit*, 2003, p. 778.
[14] S. Crook, R. Kelso, and J. Drobik, "Aeroacoustics of aircraft cavities," 2007.
[15] M. L. Shur, P. R. Spalart, M. K. Strelets, and A. K. Travin, "A hybrid RANS-LES approach with delayed-des and wall-modelled les capabilities," *International Journal of Heat and Fluid flow*, vol. 29, no. 6, pp. 1638–1649, 2008.
[16] L. Larchevêque, P. Sagaut, T.-H. Lê, and P. Comte, "Large eddy simulation of a compressible flow in a three-dimensional open cavity at high reynolds number," *Journal of Fluid Mechanics*, vol. 516, pp. 265–301, 2004.